Traffic 2013; **14:** 853–869 doi:10.1111/tra.12078

Trans-sialidase Stimulates *Eat Me* Response from Epithelial Cells

Claire E. Butler[1], Tecia M. U. de Carvalho[2], Edmundo C. Grisard[1,3], Robert A. Field[4] and Kevin M. Tyler[1,*]

[1] *Biomedical Research Centre, Norwich Medical School, University of East Anglia, Norwich, UK*
[2] *Laboratório de Ultraestrutura Celular Hertha Meyer. Instituto de Biofísica Carlos Chagas Filho, Universidade Federal do Rio de Janeiro, Ilha do Fundão, Rio de Janeiro Brazil*
[3] *Departamento de Microbiologia Imunologia e Parasitologia, Universidade Federal de Santa Catarina, Florianópolis, Santa Catarina Brazil*
[4] *Department of Biological Chemistry, John Innes Centre, Norwich, UK*

**Corresponding author: Kevin M. Tyler, k.tyler@uea.ac.uk*

Epithelial cell invasion by the protozoan parasite *Trypanosoma cruzi* is enhanced by the presence of an enzyme expressed on its cell surface during the trypomastigote life cycle stage. The enzyme, trans-sialidase (TS), is a member of one of the largest gene families expressed by the parasite and the role of its activity in mediating epithelial cell entry has not hitherto been understood. Here we show that the *T. cruzi* TS generates an *eat me* signal which is capable of enabling epithelial cell entry. We have utilized purified, recombinant, active (TcTS) and inactive (TcTS2V0) TS coated onto beads to challenge an epithelial cell line. We find that TS activity acts upon G protein coupled receptors present at the epithelial cell synapse with the coated bead, thereby enhancing cell entry. By so doing, we provide evidence that TS proteins bind glycans, mediate the formation of distinct synaptic domains and promote macropinocytotic uptake of microparticles into a perinuclear compartment in a manner which may emulate entosis.

Key words: entosis, G-protein, host-parasite, lipid raft, trans-sialidase, *Trypanosoma cruzi*

Received 28 June 2012, revised and accepted for publication 15 April 2013, uncorrected manuscript published online 18 April 2013, published online 8 May 2013

The protozoan parasite *Trypanosoma cruzi* is the aetiological agent of the tropical neglected Chagas disease, which is widespread in Latin America (1,2). In those infected, *T. cruzi* enters and proliferates amongst a variety of tissues; within epithelial and endothelial cells (3,4). Cell entry by *T. cruzi* is dramatically reduced by pertussis toxin (PT), which disrupts Gαi subunit signalling (5,6), and downstream intracellular events including reorganisation of the host cell's cytoskeleton and recruitment of vesicles to the region of plasma membrane where the parasite attaches: the parasite synapse (7–11). While the exact identity and roles of G protein coupled receptor (GPCR) ligands in Chagas disease pathogenesis remains controversial, a role for GPCRs such as the bradykinin receptor B_2, cannabinoid receptor 1 and β_1 adrenergic receptor has been well established (12–14).

GPCRs are frequently resident in lipid rafts or microdomains which are concentrated at the parasite synapse during attachment and invasion of *T. cruzi* (11); their dispersal by cholesterol depletion with methyl β-cyclodextrin (MBCD) reduces entry of *T. cruzi* into host cells (15,16). Synaptic signalling engenders increased calcium ion concentration (17,18) resulting from cross-linkage of host cell receptors, and mediated via activation of cAMP (14,19) and phosphoinositol-3-kinase (PI3K) (20). This calcium ion flux enables mobilization of lysosomes (14) and early endosomes (20) (suggesting that *T. cruzi* may utilize both exocytic and endocytic pathways) to dock with the synapse providing for parasitophorous vacuole formation. Lysosome exocytosis directs acid sphingomyelinase to the parasite synapse promoting ceramide-rich microdomain formation and increased, localized endocytic activity (21,22). This endocytic component of cell entry was highlighted by cytochalasin D (cytD) inhibition of the early fusion of peripheral lysosomes with the plasma membrane at the parasite synapse (23) which required PI3K activation (20). Caveolin-dependent endocytosis also requires PI3K activation (24,25) and caveolin-1 (cav1), has been associated with *T. cruzi* entry of macrophages (16). Cav1 which is necessary for formation of caveolae is either sequestered at the cell surface forming invaginations (26) or recycled along microtubules under the control of multiple kinases which direct caveolin delivery (25).

Trans-sialidase (TS) is a *T. cruzi* trypomastigote surface enzyme which catalyses transfer of sialic acid from host to parasite surface. Seminal work established that a single amino acid, Tyr^{342} is essential for activity (27) and that the enzyme can be entirely inactivated by point mutation at this site. Expression of TcTS itself, as well as other enzymatically inactive TS family members such as GP82, is strongly associated with virulence (28). While it is clear their roles as virulence determinants may arise from multiple functions, it is equally clear that they can act as important and specific mediators of infectivity, tropism and host cell invasion (29–31). Investigation into the role of TS during host cell entry by *T. cruzi* has described a reduction in entry upon inhibition of TS activity (32,33); however, reduced expression of some inactive members of the TS family has also been associated with reduced cell invasion (34,35). Moreover, TS activity has been implicated in roles including escape from the parasitophorous vacuole

(36), modulating host cell immunity and apoptosis (37) and cellular tropism (38); leading some to question the significance of TS activity in cell entry.

Endogenous sialidases are widely expressed in mammalian cells and increased sialidase activity is associated with epithelial neoplasia and cancer progression (39). Recently, investigations into the mechanism by which live, unanchored, epithelial cells including neoplasms are internalised by their neighbours have described an invasion-like process called entosis (40–42) documenting the constitutive ability of epithelia to take up other cells when appropriately triggered. Other studies have shown that desialylation associated with ageing and apoptosing cell surfaces can act as an *eat-me* signal promoting cell uptake by monocyte derived phagocytic cells and by microglia (43,44). We considered that TS might bind to glycosylated moieties on the host cell surface thereby cross-linking glycosyl-phosphatidylinositol (GPI)-linked glycoproteins and glycosphingolipids facilitating lipid raft formation and modulating sialylation of lipid raft GPCRs. In this manuscript, we utilize recombinant TcTS (active TS) and TcTS2V0 (inactive TS) proteins immobilized onto four micron latex beads to challenge an established model epithelial cell line, Madin-Darby Canine Kidney II (MDCK II). By doing so, we provide evidence that TS proteins bind surface glycans, mediate lipid raft formation and promote macropinocytotic uptake of microparticles into a perinuclear compartment. We find that the unique activity of this enzyme acts upon the lipid raft based GPCRs present at the synapse with the epithelial cell to promote heterotrimeric G protein signalling which in turn results in enhanced entry into epithelial cells.

Results

TS promotes bead internalization by cells

To directly examine whether TS activity has a role in cell entry, or whether the observed ability to mediate cell entry arose from other structure-related activities of the TS protein, we compared the active recombinant enzyme with a nearly identical TS disabled by a point mutation in the active site. Four micron latex beads [selected as microparticles of similar volume to the *T. cruzi* trypomastigote – circa 30 fl (45)] were coated with purified active (TcTS) and inactive (TcTS2V0) recombinant enzyme, and their TS activity was then determined using a fluorometric assay (Figure S1). The number of beads internalized by MDCK II cells following 2 h of incubation was assayed by biotinylation of the cell surface and any attached beads. Unique, arbitrarily selected fields of cells were digitally captured and all beads associated with cells were scored as attached or internalized. For each type of coated bead, two hundred cells were assayed in at least four separate experiments, and the number of beads which remained attached and internalized was compared for each protein (Figure 1). Time courses examining the kinetics with which beads coated in the active enzyme entered the cells (Figure S2) suggested that the proportion of beads taken up progressively increased over 8 h and a 2 h time point was selected for convenience. BSA and bradykinin coated beads and blank uncoated beads were used as controls.

Approximately, one third more beads coated in active enzyme (TcTS) were associated with MDCK II cells than beads coated in the inactive TcTS2V0. The proportion of beads internalized, however, was roughly similar and both were internalized in greater numbers than beads coated with bradykinin (Figure 1B), which appeared to be relatively poorly adherent but which was also able to mediate bead entry into cells. The proportion of internalized TcTS coated beads was also compared with that of BSA coated beads, however, no internalization of BSA coated beads was observed at all (Figure 1A and Table 1). Blank beads, preincubated with the culture media, were also included to control for any potential effects from serum proteins in the media that might be adsorbed onto the bead surface, however, these beads were entirely non-adherent to the cells under the conditions of these assays.

These results demonstrate that beads coated either in the active enyzme (TcTS), or the inactive TS (TcTS2V0), or the bradykinin peptide, in contrast to BSA, are able to direct uptake of microparticles by epithelial cells; but, that TS activity augments uptake relative to the inactive protein. Thus, while active and inactive TS proteins mediate proportionately similar internalization levels for the beads, the activity of the enzyme is a strong contributing factor to the sustained association between the cell and the coated bead, and hence facilitates considerably larger numbers of beads coated in active enzyme to enter epithelial cells.

TcTS activity promotes entry in a PI-3 kinase dependent manner

In corollary experiments, we investigated the role of TS activity in attachment and internalization using sialic acid acceptor substrate lactitol and pre-treating MDCK II cells with sialidase. To facilitate analysis for these and subsequent biotinylation assays, rather than capturing large numbers of arbitrary fields as described for Figure 1, 200 cells with closely associated beads were located, captured and scored as internalized or attached. Attachment of TcTS coated beads was marginally, but significantly, reduced at concentrations of lactitol greater than 0.25 mM in comparison with TcTS2V0 coated beads, where no such reduction was observed (Figure 2A). Internalization of TcTS but not TcTS2V0 coated beads was also significantly inhibited by application of (1 mM) lactitol (Figure 2B). Since lactitol is an efficient acceptor substrate of TcTS and competitive inhibitor for sialylation of acceptor substrates on the epithelial cell surface, these results suggest that attachment and internalization are facilitated by sialylation of cell surface molecules.

Interestingly, MDCK II cells treated with sialidase to remove host cell sialic acid prior to incubation with TcTS

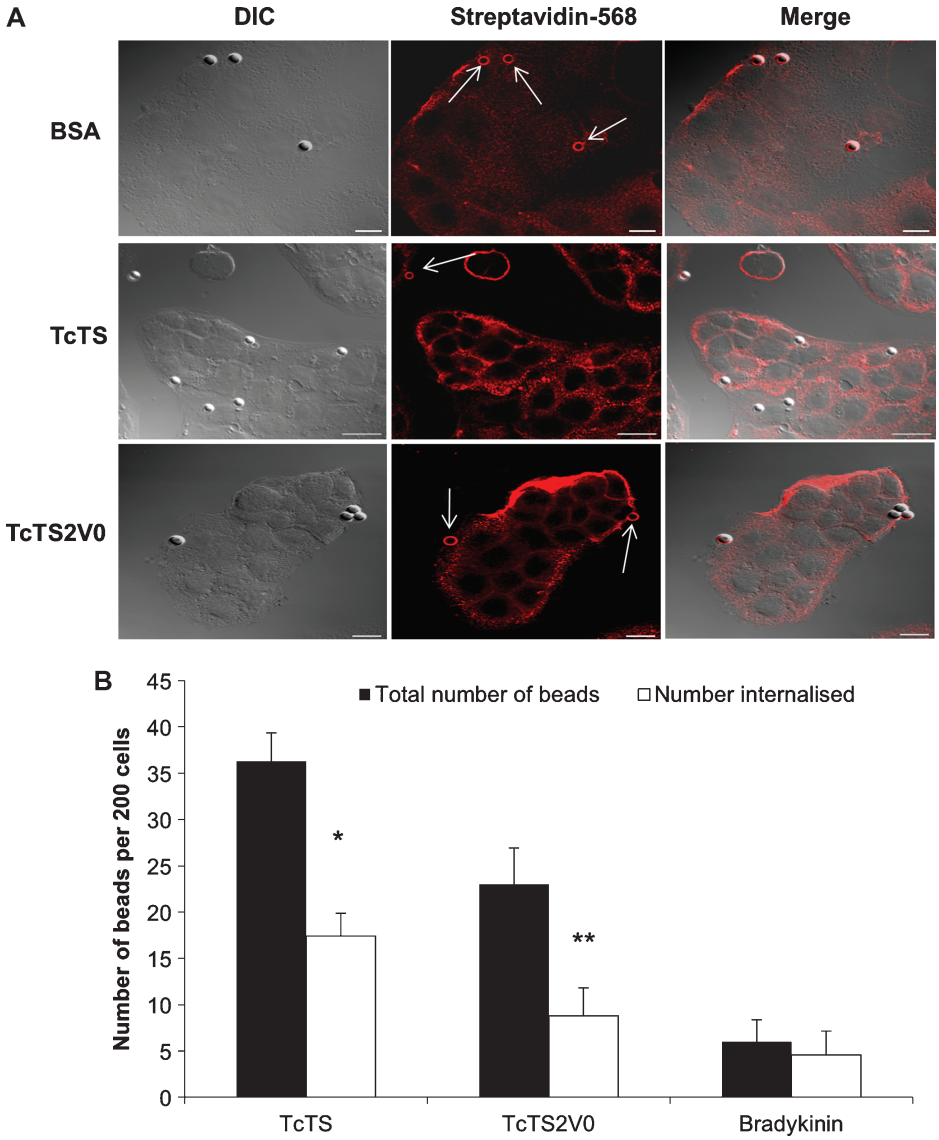

Figure 1: TcTS coated beads attach to and are internalized more effectively by epthelial cells than TcTS2V0, bradykinin and BSA coated beads. Attachment and internalization was assessed by biotinylation of the cell surface and attached beads. Beads shown in red and indicated with arrows are attached beads, where the scale bar = 10 μm (A). Protein coated beads incubated with MDCK II cells for 2 h were scored using the biotinylation assay as the number of attached and internalized beads per 200 cells (B). **p = 0.002 and *p = 0.0455 (mean ± SEM) when compared to the control ($N \geq 5$).

and TcTS2V0 coated beads actually afforded an increase in TcTS coated bead attachment (Figure 2C), but conversely showed a decrease in internalization (Figure 2D) which was not observed with the inactive enzyme. A result suggesting that while on sialidase treated cells, TcTS can bind receptors which are not influenced by sialylation; the enhanced internalization associated with the active TS is not simply a function of enhanced binding to sialylated surface proteins, or simply explained in terms of the glycan binding preferences of these proteins which are not sialic acid specific (Figure S3). Rather that enhanced internalization arises directly as a result of the trans-sialylation of specific receptors.

The release of intracellular calcium associated with *T. cruzi* entry into epithelial cells is inositol triphosphate (IP3) dependent (18) and can be prevented by treatment with PT (6), which interacts with heterotrimeric G protein subunit, Gαi. We considered whether this would also be the case for TS coated microparticle uptake. Our results demonstrate that attachment of TcTS coated beads was reduced by PT treatment whereas attachment mediated by TcTS2V0 and bradykinin was not significantly affected (Figure 2E). Correspondingly, internalization of TcTS coated beads was also partially inhibited (Figure 2F), as were bradykinin coated bead; whereas, TcTS2V0 remained unaffected. Thus, blockade of Gαi signalling

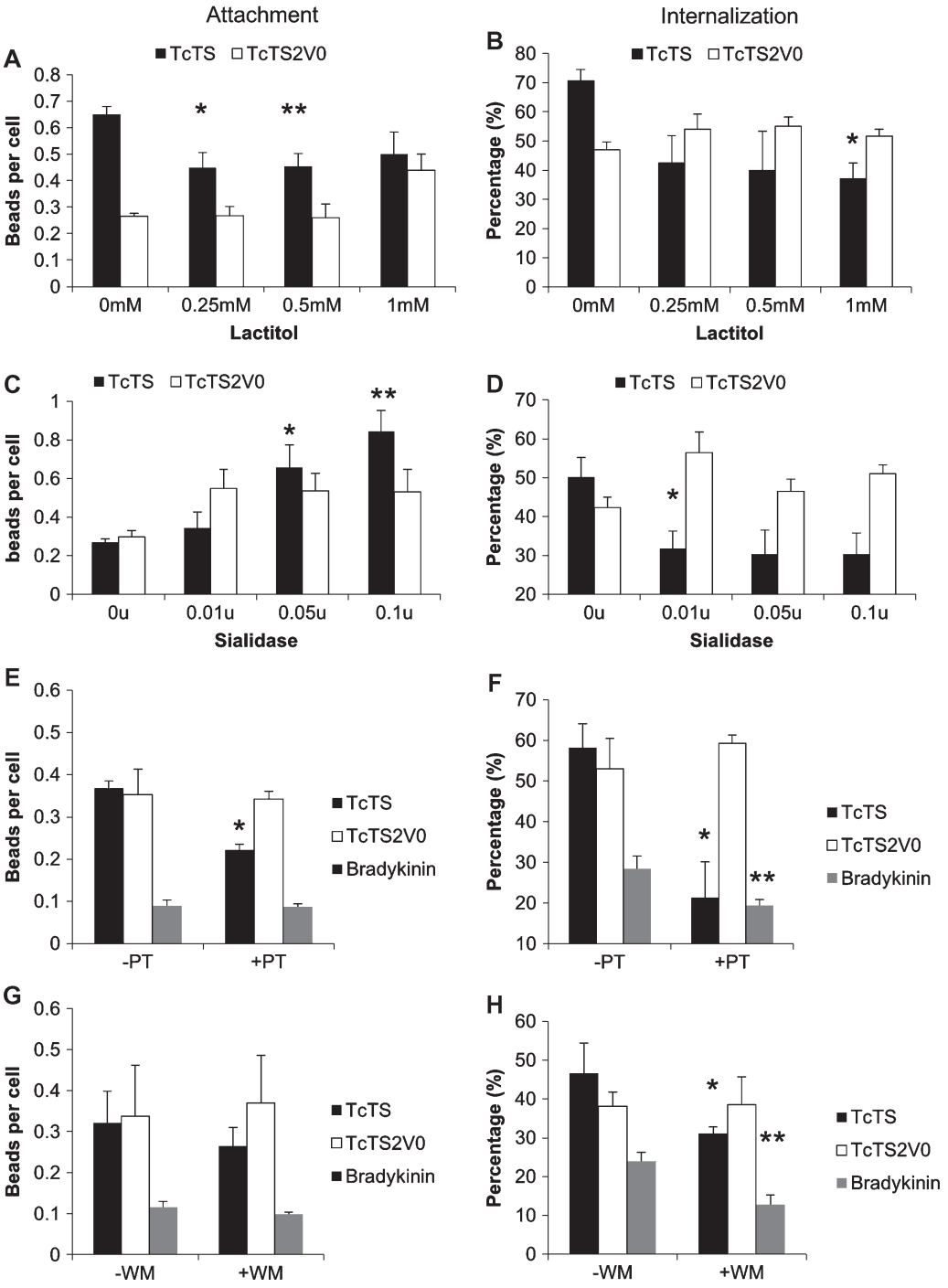

Figure 2: Inhibition of TS, Gαi or PI3K activity reduces bead internalization. TcTS and TcTS2V0 bead attachment was calculated per cell and determined post treatment with lactitol *p = 0.0349, **p = 0.0256 (A) and uptake was scored using biotinylation after incubation with lactitol *p = 0.0072 (B). Attachment of TcTS and TcTS2V0 coated beads was calculated per cell after pretreatment with sialidase *p = 0.0295 and p = 0.0061 (C) and internalization determined by biotinylation of the cell surface *p = 0.0161 (D). Attachment of TcTS, TcTS2V0 and bradykinin coated beads was also scored after treatment with PT *p = 0.0024 (E) and internalization *p = 0.0175, **p = 0.0595 (F) and wortmannin (WM) attachment and (G) internalization *p = 0.0628, **p = 0.0308 (H). Where all p values are compared to the control (mean ± SEM, $N \geq 3$).

Table 1: Epithelial cell attachment and internalization of coated beads

	Attached (%)	Internalized (%)	SD (%)
TcTS	47	53	14
TcTS2V0	57	43	15
BSA	100	0	0
Bradykinin	62	38	23

appears to specifically inhibit the TS activity mediated augmentation of bead attachment and entry rather than the process of attachment and entry overall.

Significant variation between experiments was observed in the ability of coated beads to bind cells, indicative of the sensitivity of the bead binding interaction to environmental variation. Within each independently controlled experiment though, variation was less, allowing meaningful comparison between control and treated groups. Cell cytotoxity was also assayed to show that any inhibition of internalization was due to G protein subunit inhibition and not to cell death (Figure S4A,B).

The recruitment of vesicles and the reorganisation of the cytoskeleton require the activation of PI3K (46–48), which can also occur via Gαi signalling (49). In previous studies PI3K was inhibited by wortmannin (WM) before cells were challenged with *T. cruzi* resulting in decreased cell entry and suggesting that cell invasion by *T. cruzi* requires activation of this enzyme (50). With this in mind we treated cells with WM and assessed the effect on TcTS, TcTS2V0 and bradykinin bead attachment and uptake (Figure 2G,H). Treatment did not result in a significant reduction in attachment, but did lead to a reduction in TcTS and bradykinin (but not TcTS2V0) coated beads entering the cells. Taken together these results suggest that TcTS activity stimulates PI3K signalling during cell entry via Gαi transactivation.

The internalized bead vacuole reaches a perinuclear position

We constructed an MDCK II cell line expressing both GFP-α-tubulin and cav1-RFP in order to consider the interaction between bead, microtubules and caveolin over time (Figure 3A). We observed a protracted association between cav1-RFP and TcTS coated beads; from initial recruitment to the bead synapse, through to vacuole formation and to a final destination in its perinuclear compartment. We found no increase in this association over time, however, where cav1 was initially recruited it appeared to remain in close proximity with the beads. It was apparent from this work, that at later time points beads were transported to a perinuclear position abutting the MTOC (Figure 3A). Investigation of the perinuclear compartment was undertaken with transmission electron microscopy of MDCK II cells incubated for 24 h with TS coated beads (Figure 3B). These figures clearly show the presence of the centriole juxtaposed to the bead vacuole as well as highlighting a close association between the bead vacuole and the endoplasmic reticulum (ER).

The apparent perinuclear positioning of the vacuoles containing TS coated beads seemed analogous to previous work demonstrating repositioning of the host cell MTOC in close proximity to the *T. cruzi* vacuole (10). To confirm this repositioning effect, we measured the distance between MTOC and beads in fixed cells over a 9-h time course. We found a considerable decrease in the distance between the beads and the MTOC over time consistent with bead uptake and eventual positioning in close proximity to the MTOC (Figure S5). Microtubule polymerisation is integral to repositioning of the MTOC and has also been implicated in the invasion of *T. cruzi* where tubulin appears to accumulate in the region of the attached parasite (10). To investigate whether microtubule dynamics were also associated with bead entry, cells were treated with colchicine to depolymerize the microtubules and bead entry assessed by surface biotinylation. A modest reduction in bead uptake was observed in the 5 and 10 μM range for TcTS coated beads but not TcTS2V0, while bradykinin coated beads show a decrease in internalization for all colchicine concentrations (Figure 3C). This result suggests a microtubule-dependent component mechanism in the uptake of bradykinin and active TcTS coated beads which is absent for uptake of beads coated in the inactive enzyme. Visual confirmation of microtubule depolymerisation of MDCK II cells at these concentrations was performed by colchicine treatment of GFP-tubulin expressing MDCK II cells (Figure 3D).

Polymerisation of actin is required for effective internalization of TcTS and TcTS2V0 coated beads

Host cell invasion is often associated with cytoskeletal remodelling and *T. cruzi* has been proposed to invade epithelia by both tubulin and actin dependent mechanisms. Previous studies have described *T. cruzi* mediated depolymerisation of the cortical actin cytoskeleton in some cells (9) and induction of actin-rich pseudopodia (51,52). In this study, TcTS, TcTS2V0 and bradykinin coated beads were incubated with MDCK II cells before immunolabelling for β-actin. The resultant images show ruffling; with cup-like actin-rich projections closely associated with the beads, and in some cases surrounding them entirely (Figure 4A). Interestingly, this activity appeared to be independent of TS activity, as it was also observed when beads were coated with TcTS2V0 (Figure 4B). We inhibited microfilament polymerization with cytD prior to the addition of TcTS, TcTS2V0 and bradykinin coated beads. In each case this treatment almost entirely inhibited bead internalization even at low concentrations (Figure 4C), confirming a role for microfilament dynamics in microparticle uptake which did not relate to TS activity *per se*. The cytD treated cells were stained for β-actin after treatment to evaluate the extent of depolymerisation at each concentration (Figure 4D).

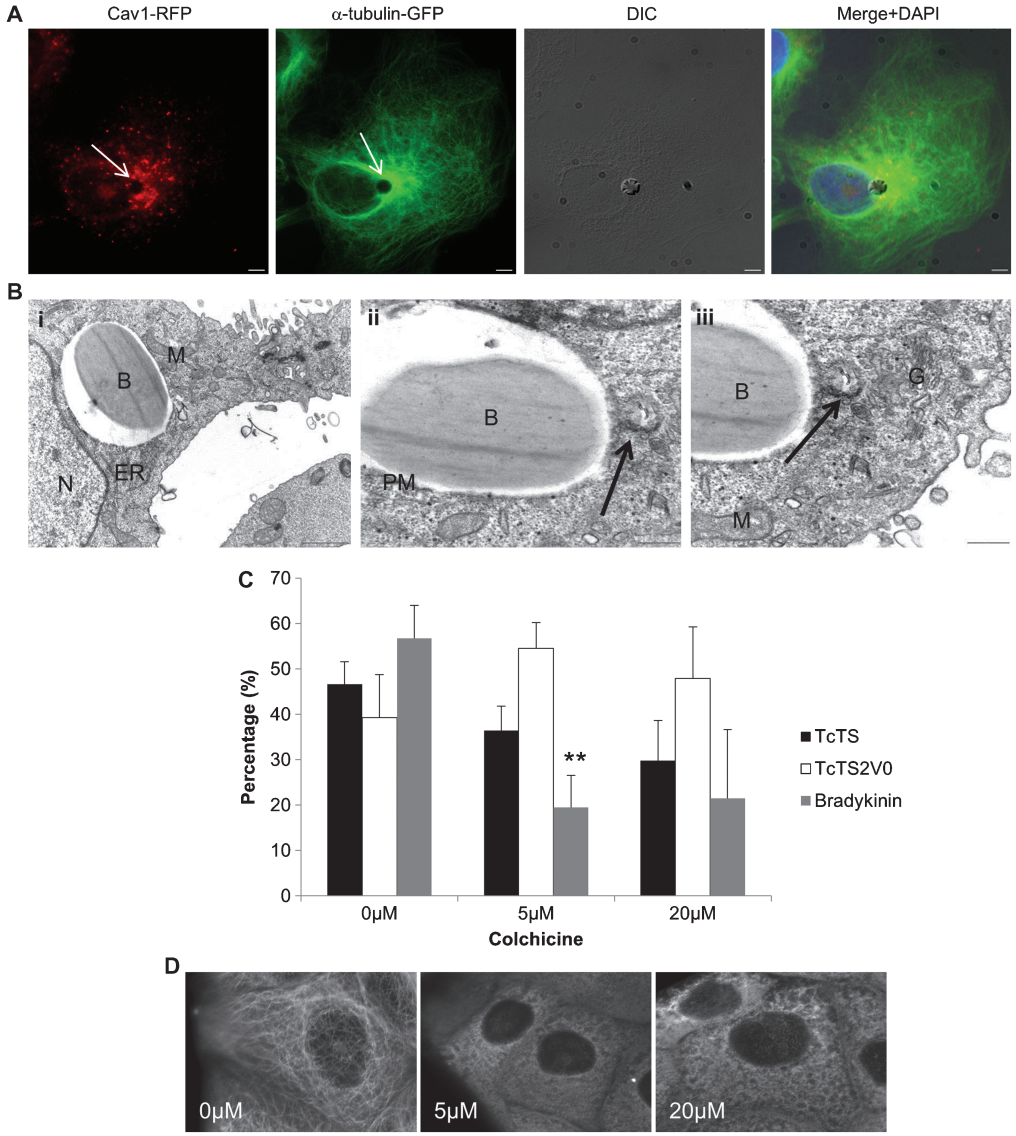

Figure 3: Microtubule dynamics in perinuclear positioning of internalized microparticles. Beads coated with TcTS (DIC) were incubated with MDCK II cells stably expressing GFP-tubulin (green) and cav1-RFP (red) for 6 h. The arrows indicate the position of the bead, scale bar = 5 μm (A). MDCK II cells were incubated overnight with TcTS coated beads before preparation for transmission electron microscopy (B). The 4 μm white beads are shown here in close proximity to mitochondria (m), golgi (G) and ER, scale bar = 1 μm (i). The centrosome (arrow) is also visible in very close proximity to the bead, scale bar = 0.5 μm (ii). Close to the centriole the golgi is clearly visible, scale bar = 0.5 μm (iii). B-bead, PM-phagosomal membrane and N-nucleus. MDCK II cells were incubated with 0, 2, 20 μM of colchicine to depolymerize microtubules before incubating with TcTS, TcTS2V0 and bradykinin coated beads for 3 h. The number of internalized TcTS coated beads was determined by biotinylation (mean ± SEM, $N = 3$, **p = 0.008) (C). MDCK II cells expressing GFP-tubulin were imaged after application of the indicated concentrations of colchicine (D).

Cell cytoxicity was ruled out as a cause for the decrease in internalization by LIVE/DEAD® assay where cell death remained at a basal rate despite addition of the drug (Figure 4E).

Cav1 is recruited to internalized beads and parasites but is not essential for internalization

A significant proportion of cell invasion by *T. cruzi* into epithelial cells is dependent on formation of a host cell plasma membrane-derived vacuole (20). To determine if the observed TcTS-mediated internalization of coated beads was similarly associated with plasma membrane markers we looked for evidence of association with a canonical marker from one of the major endocytic pathways – cav1. Immunofluorescence at short timepoints showed that many of the attached beads coated with both TcTS and TcTS2V0 were associated with increased concentration of cav1 (Figure 5A).

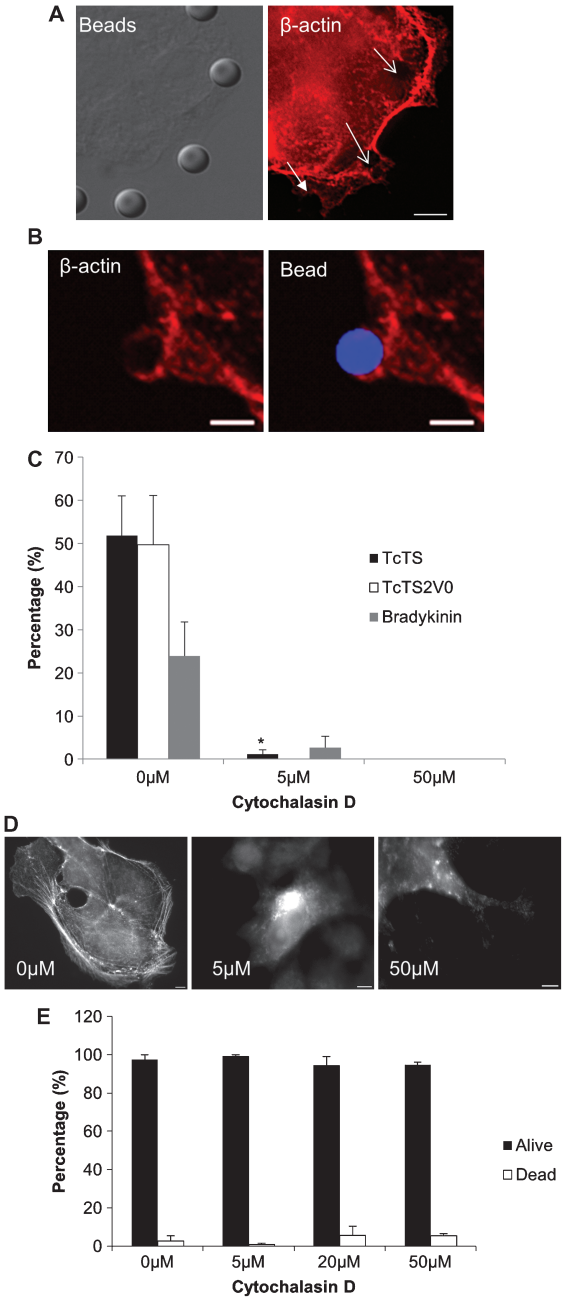

Figure 4: Bead internalization is actin dependent. MDCK II cells were incubated with TcTS (A) and TcTS2V0 (B) coated beads. The position of the beads is shown with DIC and arrows (A) and blue fluorescence (B). Immunolabelling with anti-β-actin (red) shows ruffling and increased concentration associated both kinds of coated beads after labelling with anti-mouse Alexa Fluor568. Scale bar = 5 μm. Biotinylation assay for bead internalization demonstrated that treatment with cytD completely prevents bead internalization after 3 h (C). Depolymerisation of microfilaments was confirmed by immunolabelling with anti-β-actin after treatment with 0, 5, 50 μM of cytD, scale bar = 5 μm (D). The level of cell cytotoxicity after addition of cytD was assayed by LIVE/DEAD® assay (E). Graphs show mean ± SEM ($N = 3$) where $^{**}p = 0.0007$ and $^{*}p = 0.049$ when compared with the untreated control.

Previously, an association with cav1 has been described with *T. cruzi* invasion of macrophages (16) but its role in epithelial cell invasion has not been explored. We, therefore, considered whether live parasites attached to epithelial cells recruited caveolin to the parasite synapse. We found that attachment of trypomastigotes often resulted in a marked increase in cav1 at the parasite:cell synapse (Figure 5B), implying that attachment might promote cav1 translocation. We found this association irrespective of the parasite strain or epithelial cell line we used (not shown). We also noted that at a longer (6 h) time point, as many as half of the vacuoles formed remained associated with caveolin regardless of whether live or killed parasites, or beads were used (Figure 5C).

In light of its association with TcTS coated beads we considered whether cav1 might play a functional role in TcTS-mediated epithelial cell entry. We silenced cav1 expression in MDCK II cells, reducing expression levels by more than 90% (Figure 5D,E). The proportion of TcTS coated beads internalized by silenced cells showed no significant difference to unsilenced controls (Figure 5F). A result which suggests that although caveolin is a plasma membrane marker which is enriched at the bead synapse, it is present primarily as a bystander and that caveolin-dependent endocytosis is not a mechanism which promotes entry of TcTS coated beads into epithelial cells *per se*.

TcTS coated bead attachment is inhibited by cholesterol depletion

Cholesterol is an essential component of the lipid containing assemblies of the plasma membrane (53) and specific extraction of cholesterol from the plasma membrane by MBCD results in the dissipation of these assemblies. Previously, depletion of cholesterol has been shown to inhibit the ability of *T. cruzi* to invade cells (15), suggesting the integrity of these domains is important for cell entry by *T. cruzi*. To investigate the effect of removing cholesterol on attachment of TcTS and TcTS2V0 coated beads we considered whether the number of attached beads was reduced by treatment of the cells with MBCD. We found that attachment of both TcTS and TcTS2V0 coated beads to MDCK II cells was modestly, but significantly impaired by treatment with MBCD (Figure 6A), suggesting epithelial adhesion cell is favoured by concerted interaction with surface moieties tethered to cholesterol-dependent assemblies in the plasma membrane. Interestingly, the removal of serum from the media enhanced binding by beads coated in the active TcTS (perhaps by promoting contact with donor and acceptor substrates on the cell surface), but actually afforded reduced binding by beads coated in the inactive TcTS2VO.

TcTS activity-independent entry is serum sensitive

In testing the cholesterol dependence of internalization of both TcTS and TcTS2V0 coated beads, we aimed to

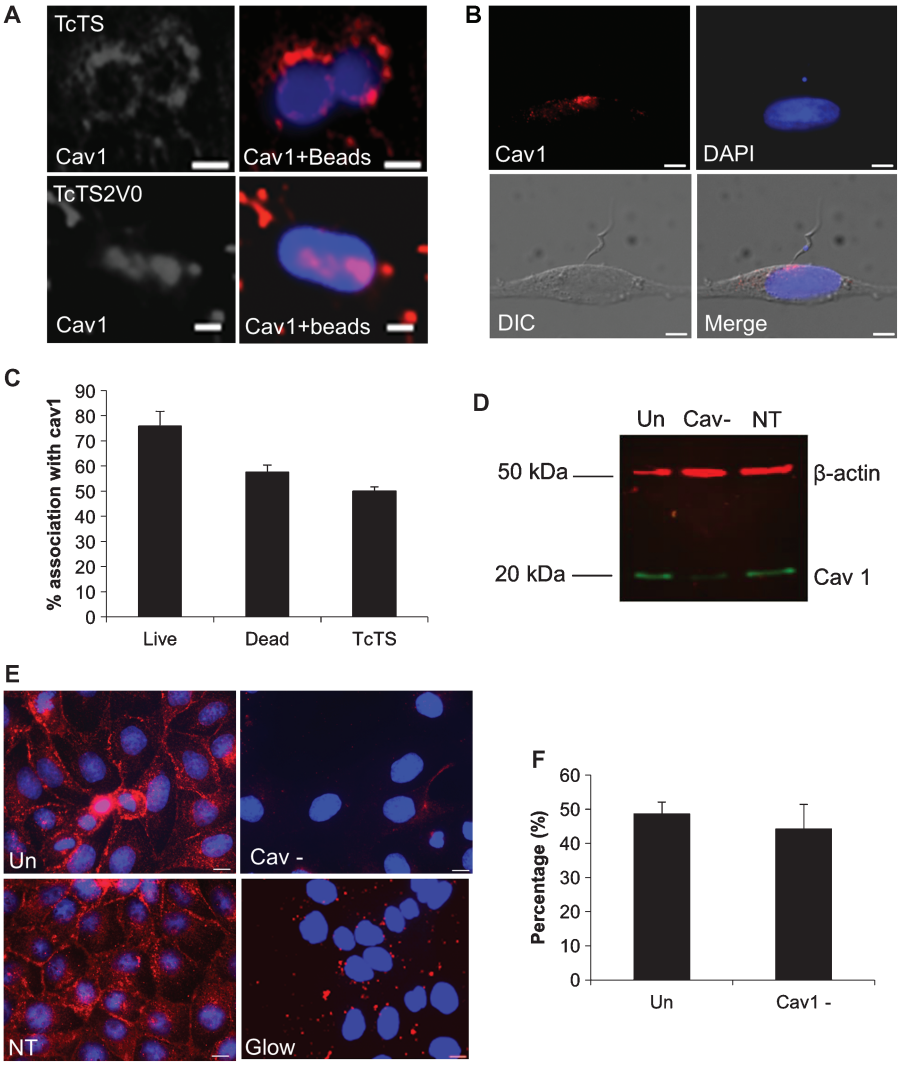

Figure 5: Caveolin-1 is recruited to bead and parasitophorus vacuoles in epithelial cells but reduced cav1 expression does not affect bead internalization. For MDCK II cells incubated with TcTS and TcTS2V0 coated beads and immunolabelled with anti-cav1 antibody, cav1 accumulates in close proximity to attached and internalized beads. Scale bar = 2 μm (A). Live parasites used to infect OK cells show considerable concentrations of cav1 at the parasite synapse during attachment (B). The scale bar = 5 μm. Most vacuoles of TcTS coated beads, live and dead parasites associate with cav1, but the association is strongest for live parasites (C). MDCK II cells were transfected with cav1 siRNA (Cav-) and non-targeting siRNA (NT) and separated by SDS-PAGE before transferring by western blot. The resultant membrane was labelled with anti-cav1 (green) and anti-β-actin (red) antibodies, untransfected cells (Un) were also run alongside and the membrane was imaged using an Odyssey® infrared imager (D). The transfection rate was calculated by immunolabelling cells with cav1 antibody and transfecting with glowing RNA (E), scale bar =10 μm. Untransfected and transfected cells were biotinylated and imaged by confocal microscopy after incubation with TcTS coated beads for 2 h. (graphs show mean ± SEM, $N \geq 3$) (F).

assess the uptake of the beads from MBCD treated cells compared with untreated cells. The use of MBCD requires that cells are assayed in the absence of sera supplements and we compared bead uptake in cells treated with 10, 20 and 30 mM of MBCD for an hour with that in cells simply exposed to sera free media for the same period and cells in normal media containing Foetal Calf Serum.

We observed a dramatic decrease in internalization of TcTS2V0 beads even without MBCD treatment in the absence of sera (>95% reduction). The absence of sera also reduced the internalization of TcTS beads but this effect was considerably less profound, with significant numbers of TcTS beads still internalized. TcTS and TcTS2V0 coated bead internalization was further inhibited by increases in MBCD concentration until internalization and was completely blocked at 30 mM (Figure 6B). A live/dead cell assay showed that MBCD had cytotoxic effects only at 30 mM and above (Figure S6). These results confirm that internalization of TcTS and TcTS2V0 coated beads is cholesterol dependent, relying on the cholesterol containing assemblies of the plasma membrane. Strikingly

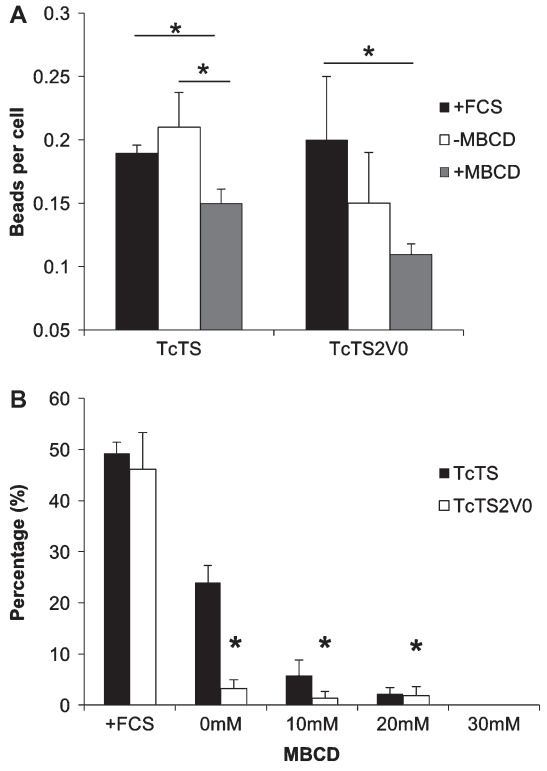

Figure 6: Cholesterol depletion prevents internalization by both TcTS and TcTS2V0 coated beads. Internalization of coated beads was assessed using the biotinylation assay. The level of attachment is shown with FCS and before and after treatment with MBCD for both TcTS and TcTS2V0 coated beads (A) (mean ± SEM) where *$p < 0.05$. The effect on protein coated bead internalization by 10, 20 and 30 mM of MBCD was also assayed and compared with untreated cells which had and had not been deprived of serum (B) (mean ± SEM, *$p < 0.05$).

though, the differential susceptibility to serum depletion we observed further uncouples the mechanism by which TS activity augments uptake of the beads coated in active enzyme, from the serum sensitive macropinocytotic mechanism by which TS proteins can direct cell entry in an activity independent manner.

The bead-cell synapse membrane shows increased lipid order

Actin dependent uptake from the plasma membrane and the presence of caveolin at the bead's interface with the cell imply localized structuring of the plasma membrane. Lipid rafts can be defined as regions of the cell membrane which exhibit increased lipid order, being tightly packed and enriched with sphingolipids and cholesterol. Lipid rafts can often be detected at the synapses between cells (54) or between cells and pathogens (55) as cross-linkage of GPI linked glycoproteins or glycosphingolipid receptors is believed to be sufficient to serve as a driver for a localized increase in membrane order. Visualization of these regions can be achieved by use of the dichromatic dye Laurdan and localized quantification of membrane order in the cell using Laurdan on a widefield microscope can be achieved by computation of the generalized polarisation (GP) value (56). The GP is the normalized intensity ratio between the two emission channels where the maximum +1 is the most condensed and the minimum −1 is the most fluid. When these values are mapped onto micrographs, cell membrane which appears 'warmly coloured' represents regions of high lipid order, while regions that appear in the blue end of the spectrum are less well ordered. We used this dye to examine whether the regions of plasma membrane where TcTS and TcTS2V0 coated beads had attached showed evidence of increased lipid order indicative of the ability of such proteins to cross-link glycolipids and glycoproteins.

Images were collected separately at emissions of 435, 460 and 500 nm using a dichroic mirror block to obtain triple split images, the 435 and 460 nm images were combined as previously described (56,57) to produce a final GP image (Figure 7A). TcTS coated beads were found to lie in contact with regions of the cell surface membrane which appeared more ordered than the rest of the cell (yellow, orange and red pixels). Such regions were present throughout the cell surface but appeared to accumulate proximal to the beads. The same phenomenon was observed with the TcTS2V0 coated beads which also appeared to attach via more warmly coloured regions.

Using SimFCS software, the GP was calculated for each pixel in a 30×30 pixel square region of interest (ROI) encompassing the bead synapse and for an equivalent ROI from the same cell in close proximity (Figure 7A). Histograms were produced showing the spread of GP values, control ROIs exhibited more negative average GP value (−0.099) than the ROI in contact with a TcTS coated bead (+0.003) (Figure 7B). The same patterns are also shown when TcTS2V0 coated beads are attached to the cell membrane (Figure 7C) with a visible shift in average GP from −0.013 to +0.136 in contact with the bead. Comparison of multiple ROIs of membranes in contact with the protein coated beads show that the region of membrane in contact with both TcTS and TcTS2V0 coated beads is more ordered than the regions of membrane not in contact with either protein coated bead (Figure 7D). Importantly however, no discernible difference was observed in the increased GP values from active and inactive enzyme, suggesting that the ability to cross-link host surface proteins and induce raft formation at the bead synapse are similar. Lending support to this observation, we found only relatively minor differences between the glycan binding profiles of the active and inactive enzyme (Figure S3). Those significant differences that were observed were not all or nothing, but rather showed differential avidity for fucose, mannose, lacto-*N*-biose I and sialic acid. Interestingly though, some of these glycans are associated with mucins which are GPI-linked. Our results are consistent with lipid raft formation at the bead synapse and suggest that attachment of both TcTS and TcTS2V0 coated beads (through cross-linking of glycosylated

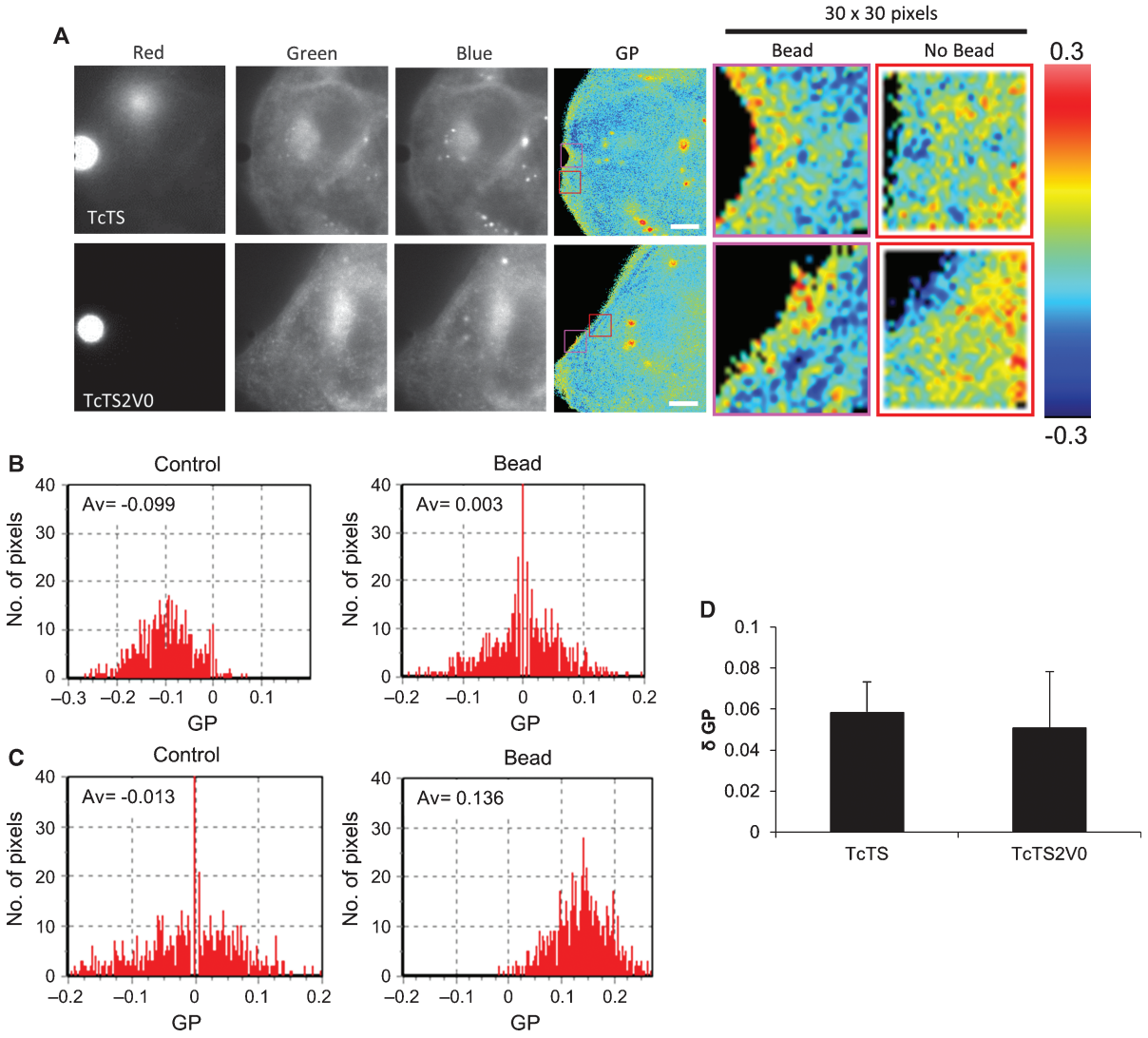

Figure 7: TcTS and TcTS2V0 coated beads attach to microdomains with increased lipid order. MDCK II cells were imaged using triplesplit dichromatic mirrors showing the red, green and blue wavelengths. The individual images were then aligned in IMAGEJ and a final ratio image produced in SimFCS to give a colour representation of membrane order. Regions of the cell membrane of higher order are shown in red, orange and yellow. Regions of the cell membrane in contact with TcTS and TcTS2V0 coated beads were imaged (scale bar = 4 μm) (A). The GP calculated for each pixel in a 30 x 30 pixel box for control regions of the cell membrane (shown in the red boxes with the corresponding ratio image) and regions in contact with TcTS and TcTS2V0 coated beads (shown in the pink boxes) and the corresponding histograms plotted for TcTS (B) and TcTS2V0 (C) show a marked increase in GP from the bead interface. When such change in GP is compared between beads coated in active and inactive enzyme no significant difference is observed both appearing to exert a similar degree of structuring influence on the membrane (mean ± SEM, N = 5) (D).

moieties on host glycoproteins and glycolipids) lead to structuring of an epithelial cell synaptic membrane characterized by regions of high lipid order which do not form when cholesterol is depleted (Figure S7A,B).

Discussion

Penetrating and replicating within mammalian epithelia and other non-phagocytic cell types is integral to the life-cycle of *T. cruzi*. As part of the arsenal evolved by the parasite to facilitate infection, trypomastigotes express several members of the *T. cruzi* TS family which have been previously implicated in host cell invasion, including some, such as gp30 and gp82, which have been shown to induce intracellular Ca^{2+} ion release (58,59). Here, we have demonstrated that while TS activity may not be necessary for cell entry, it does possess the ability to enhance entry into epithelial cells. This is in accordance with data previously presented demonstrating the reduction in *T. cruzi* internalisation after treatment with lactitol and after host cells were treated with sialidase to remove sialic

acid (32,33). Furthermore, here, we show that purified recombinant TS alone can potentiate similar responses from the host cell as the whole parasite; and moreover, that the presence of a homogenous coating of inactive recombinant TS protein is sufficient to mediate efficient epithelial cell entry.

We observe a reduction of the distance between TS coated beads and the MTOC with time which is accompanied by an enrichment of tubulins around the bead vacuole. This correlates closely with the behaviour observed during formation of the parasitophorous vacuole of *T. cruzi*, where microtubule rearrangement and nucleation of microtubules from the vacuole was observed and in which GFP-tubulin expressing MDCK II cells also implicated the host centrosome in the internalization of *T. cruzi* by suggesting that it migrates towards the nascent parasitophorous vacuole (10). The final proximity of the bead vacuole to centrosome may imply that as with *T. cruzi*, the internalized bead is able to affect host cell microtubule dynamics and influence positioning of the MTOC. Alternatively, bead vacuoles may be actively transported by motors such as kinesins to a perinuclear location in a manner analogous to that observed for several other pathogens (60). *Toxoplasma gondii* infected cells also exhibit translocation of the centrosome and microtubules appear to shorten around the parasitophorous vacuole (61), facilitating bidirectional motion of vesicles. The host cell membrane at the *T. cruzi* parasite synapse and membrane of the *T. cruzi* parasite vacuole is able to act as an MTOC rapidly recruiting gamma and tyrosinated tubulins which polymerize into microtubules (10). Similarly, in the absence of the host centrosome, the parasitophorous vacuole of *T. gondii* can also act as an MTOC, enabling the formation of microtubules around the parasitophorous vacuole (62).

The vacuole formed by TcTS coated beads appears qualitatively different to that associated with apicomplexan parasites such as *T. gondii*. *Toxoplasma gondii* has recently, however, been shown to ligate sialic acid via microneme adhesive repeat (MAR) domains of some of their micronemal repeats like MIC1, which may be analogous to ligation of sialic acid by the TcTS (63,64). For *T. gondii* a sorting junction excludes certain components of the host plasma membrane during vacuole formation and in particular cav1 is specifically excluded from the parasitophorous vacuole. Nevertheless, the vacuoles of *T. gondii* and the TcTS coated beads are found in perinuclear positions in proximity to the centriole, mitochondria and golgi (62,65). An even more striking observation is the close association with ER which is reminiscent of the *T. cruzi* and *Leishmania* sp. vacuoles (66) and has been linked to autophagosome formation (67).

Both TcTS and TcTS2V0 coated beads formed synapses with the host cell plasma membrane which exhibited a higher lipid order when compared to the surrounding membrane and assessed using generalized polarity mapping for the lipophilic fluorophore, Laurdan. This implicates lipid rafts in the initial attachment of TS, suggesting that the receptors for TS are either located in microdomains or that they translocate there upon cross-linkage by the enzyme. The role of lipid rafts in epithelial cell invasion for other intracellular pathogens such as *Shigella flexneri* and *Salmonella typhymurium* is well established and requires the type II secretion system for cell entry where their primary entry molecules IpaB/SipB (respectively) bind directly to cholesterol prior to engulfment (68). *Salmonella* adhesion to gut epithelia is mediated via the glycan fucose (69) and it is therefore interesting that we find that *T. cruzi* TS also binds strongly to fucose moieties irrespective of activity (Figure S3).

Lipid rafts are also termed signalling platforms due to the clustering of receptors and are essential for a range of pathogens. Previous support for lipid raft formation at the *T. cruzi* synapse comes from studies showing an accumulation of raft markers such as GM1 ganglioside, LDLr, AKT-PH-GFP and the cannabinoid receptor associated with invading *T. cruzi* (13,15,20,70). In this study, we observe considerable recruitment of the canonical lipid raft marker cav1 by both trypomastigotes and coated beads during internalization. We utilized RNA silencing of cav1 to investigate whether the observed accumulation at the bead synapse was integral to bead internalization. Although we were able to silence cav1 effectively in our epithelial cell cultures, we found no evidence that reducing cav1 expression led to inhibition of bead entry. It seems most likely therefore, that during TcTS-mediated cell entry, caveolin is recruited as a bystander to the micro-environment formed when TcTS binds to host cell receptors, but that cav1 plays little if any role in the uptake of TcTS coated beads *per se*. This result echoes previous experiments where trypomastigote invasion into fibroblasts from cav1 knockout mice appeared largely unaffected by the loss of the gene (71).

Lipid rafts and actin dynamics are closely associated, particularly in regard to endocytic processes (72) and actin has been identified as an important component of the *T. cruzi* cell invasion process. Actin dynamics are already known to play a critical role in parasite entry, early lysosomal fusions and parasite retention (23); moreover actin-rich structures and actin-like projections associated with trypomastigote entry have previously been described (51,73). Our results indicate that actin is vital for the internalization of beads and that polymerisation of actin in the region of the bead is observed in association with formation of pseudopodia-like structures which may be a common requirement for uptake of microparticles. Membrane ruffling has been observed during the internalization of polystyrene beads coated in transfection reagents and in this case, upon entry, the beads associate with acidic endosomes and then with the LC3 autophagy marker (74), a marker which has also been previously associated with the *T. cruzi* vacuole (67) and entotic vacuoles (40).

The evidence presented here regarding the mechanism of cell entry by coated beads comprises lipid raft formation, cholesterol and actin dependency for coated bead uptake, lack of association with clathrin, failure of cav1 silencing or microtubule depolymerisation to prevent internalization, serum sensitivity and finally, observation of actin pseudopodia and microfilament accumulation around the beads during uptake. Even in the absence of TS activity, TSs are able to mediate cell entry and our results indicate that this ability is acutely dependent on the presence of serum in the medium. We have not resolved the reasons for this dependency, however, it is consistent with the observed reliance of macropinocytosis on the presence of exogenous growth factors which are supplied in the serum (75). Taken together our evidence suggests that macropinocytosis is the mechanism of entry for TS coated macroparticles and consistent with this it is also a mechanism that has also recently been reported for *T. cruzi* entry (76).

We have shown in this manuscript that immobilization of TS activity on microparticle surfaces serves to direct the activity to a synaptic region of the host cell plasma membrane where the activity results in activation of G proteins facilitating cell entry of the coated microparticles. Within the synapse formed, TS activity promotes redistribution of sialic acid by desialylation of donors and trans-sialylation of acceptors. Consistent with this, where activity is inhibited, or the cell surface is first sialidase treated, the effect of TS activity on bead uptake is reduced. Previous work has suggested roles for GPCRs; bradykinin-2 receptor, beta-adrenergic receptor-1 and cannabinoid receptor-1 (12–14). These proteins are heavily glycosylated and potentially may be activated as a result of sialic acid transfer resulting in the activation of G protein-dependent signalling events. Indeed the evidence which links the bradykinin-2 receptor to *T. cruzi* cell entry (12) coupled with recent work which shows that sialylation of this receptor stabilizes its retention at the cell surface and facilitates its dimerization thereby potentiating Gαi signalling (77,78) makes it possible that the bradykinin-2 receptor is a target of TS activity; serving as a sialic acid acceptor. Trans-sialylation by TcTS has previously been linked to activation of signalling activity when CD43, a highly sialylated mucin, was demonstrated as an acceptor substrate able to induce apoptosis in thymocytes (37); implying that the role played by TS at the cell surface may be cell-type dependent and highly complex. PT inhibits the Gαi subunits of heterotrimeric G proteins by preventing the interaction between the G proteins and the GPCRs on the cell surface, negatively controlling the activation of cyclic AMP (79), and eliciting downstream effects on vesicle recruitment to the cell surface. This in turn may influence the composition of the synaptic membrane, potentially increasing microdomain formation through the action of the acid sphingomyelinase (21).

Several other *T. cruzi* molecules have been implicated in the production of an intracellular rise in calcium ions, which drives parasite invasion. Oligopeptidase B has the capacity to release an extracellular molecule that can induce an IP3 dependent mechanism of intracellular calcium release (19). The intracellular rise in calcium is detected by synaptotagmin VII which in turn regulates vesicle docking with the plasma membrane which aids parasite invasion (80). A distinct internalization pathway has also been described which is readily inhibited by the PI3-kinase inhibitor WM (20), and we have found that enhanced cell entry mediated by TS-activity may also be influenced by the activity of the PI3-kinase. The signalling pathways utilized by different *T. cruzi* strains to enter epithelial cells can vary (81) and *T. cruzi* TSs are highly polymorphic in sequence and expression levels, so it is worth considering that those strains with higher TS activities will be more able to make better use of this pertussis-sensitive mechanism for enhancing cell entry and may be better at invading epithelial cells than strains with trypomastigotes that possess lower TS activities.

Epithelia represent natural barriers to infection and the cells which compose them are usually considered to refrain from phagocytosis of larger bodies such as parasites, bacteria or latex beads. They are though acknowledged to be able to take up unanchored neoplastic cells by a process known as entosis. Moreover, up-regulation of endogenous surface sialidases such as Neu 3 is firmly associated with neoplasia (39). Here, we show that epithelia can also internalize microparticles coated with TS (and bradykinin) in a similar fashion. This process is enhanced (through the action of the TS) by the localized removal of sialic acid to as yet unknown acceptor substrates. This action appears to engender a pertussis and WM sensitive *eat me* signal that results in enhanced macropinocytotic uptake. Thus like entosis, this mechanism appears macropinocytotic and enhanced by PI-3 kinase activation (40). Whether this activation is sensitive to the removal of sialic acid has not been investigated here, however sialic acid-binding lectins have been shown to inhibit PI3K autophagy pathways (82) and autophagy plays a key role in the efficient invasion of cells by *T. cruzi* into parasitophorus vacuoles containing LC3 (67).

In summary, we observe here that TS mediated macropinocytotic internalization of coated microparticles is modulated by G protein activation, suggesting that sialic acid transfer activates the GPCRs which regulate the process. We further postulate that TS mediated uptake by epithelia may have arisen by emulation of entotic *eat me* signals generated by endogenous sialidases and evolved as part of a surveillance system for epithelial neoplasms.

Materials and methods

Drugs and reagents

Red, blue and blank sulphate-modified latex beads (4 μm) were purchased from Molecular Probes® (Invitrogen). The Sulfo-NHS-LC-biotin and BCA protein assay kit were purchased from Pierce. The inhibitors and cholesterol chelators; MBCD, WM, sialidase (*Vibrio cholerae*), lactitol, cytD, co and PT

were purchased from Sigma-Aldrich. Antibiotics G418, hygromycin B and amphotericin B were purchased from Invitrogen.

Antibodies

The anti-Trypanosome Alpha Tubulin (TAT) antibody was a kind gift from Prof. K. Gull (Oxford University, UK) and rabbit polyclonal to cav1, caveolae marker and rabbit polyclonal to beta actin were obtained from Abcam. Monoclonal anti-polyhistidine peroxidase conjugate clone His1 and monoclonal anti-β-actin clone AC-15 (western blot experiments) were purchased from Sigma-Aldrich. IRDye 680RD goat anti-mouse IgG (H + L) and IRDye 800CW goat anti-rabbit IgG (H + L) were obtained from LI-COR Biosciences. Streptavidin conjugated Alexa Fluor® 568 was purchased from Invitrogen while streptavidin conjugated Cy3 was purchased from Caltag Medsystems. Green-fluorescent Alexa Fluor-488 and red-fluorescent Alexa Fluor 568 conjugated anti-mouse IgG (H + L) and red-fluorescent Alexa Fluor 568 conjugated anti-rabbit IgG (H + L) were all purchased from Invitrogen.

Recombinant proteins and activity analysis

The expression plasmids containing polyhistidine tagged TcTS and TcTS2V0 were kindly supplied by S. Schenkman and A.C.C. Frasch, respectively. The TcTS was a 70 kDa compound truncated at the C terminus to remove the SAPA repeat unit while maintaining the TS activity (83) while TcTS2V0 has a Tyr^{342}-His substitution (27). The DH5α *E. coli* strain was used to express the proteins which were induced using 1 mM IPTG and grown shaking for 3 h at 27°C. Cells were lysed in 1× binding and wash buffer made as per the manufacturer's instruction (Invitrogen) with lysozyme (1 mg/mL) and then sonicated. Purification was achieved by incubating *Escherichia coli* lysates with Dynabeads® His-tag (Invitrogen) as per the manufacturer's instructions; eluates were kept at 4°C until use. Purification samples were separated using SDS–PAGE and the protein bands visualized using SYPRO® gel stain (Invitrogen). Latex beads were coated with TcTS and TcTS2V0 at concentrations determined by BCA assay or with bradykinin and BSA as determined by the manufacturer (Sigma). To coat the beads a 10% bead solution was made in PBS and washed twice. The protein was then added to the desired concentration and allowed to coat the beads overnight under agitation at 4°C. The beads were then centrifuged and washed in PBS twice to remove surplus protein and resuspended in PBS or sample loading buffer (SLB). Immunoblotting was performed on 10 μL of coated beads and an anti-His antibody was used to confirm identity of the purified protein.

TS activity was assayed as previously described by Schrader and colleagues (84) and adapting the protocol to a 12 well plate. Samples were screened using a BMG-labtech fluostar plate reader at 350 nm (ex) and 460 nm (em).

Cell culture and labelling

MDCK II cells were maintained in DMEM supplemented with 10% Foetal Calf Serum, 5 mM L-glutamine, 50 μg/mL streptomycin and 50 units/mL penicillin. OK (Opossum Kidney) cells (HPACC) were maintained in IMEM and supplemented as described above. Cells expressing GFP-tubulin were a kind gift from Dr. Mette Mogensen (University of East Anglia, UK) and were supplemented with G418 (100 μg/mL).

Prior to experimental procedure, cells were seeded into 12 well plates containing 13 mm diameter coverslips to a density of 8×10^4 cells per mL and grown for approximately 20 h at 37°C. Cells were fixed with 3% PFA and permeabilized with 1% NP40. The actin cytoskeleton was visualized using anti-β-actin antibody and cav1 vesicles with anti-cav1 antibody after blocking with 10% neutral goat serum.

Attachment and internalization assays

MDCK II cells were seeded as described above, 1.4×10^4 protein coated beads were then added to the cells and centrifuged for 1 min at 300 × ***g***. The plate was returned to a 37°C incubator for 2 h before the media was removed and the cells were rinsed in PBS and biotinylated as previously described (85). For the inhibitor studies, cells were treated as previously described and incubated with beads for the following times: PT, 2 h (86); sialidase, 1 h (33); CytD and Co, 3 h (87). 20 nm of WM was incubated with cells for 30 min prior to addition of beads for 2 h, cells were incubated with MBCD and beads for 1 h and lactitol was added to the media with the beads at concentrations of 0.25, 0.5 and 1 mM and incubated with the cells for 3 h.

Biotinylation was assayed by confocal microscopy and the percentage internalization was assayed as the ratio of the number of beads in cells which were unbiotinylated (internalized) to biotinylated beads clearly associated with cells surface (attached) where the ratio was expressed as a percentage of total cell-associated (bound and internalized) beads. Attachment and internalization values were derived from scores of 200 cells with attached and/or internalized beads from digitally captured fields. Fields were captured either arbitrarily to avoid normalizing bias in comparisons of absolute numbers of beads attached or internalized (Figure 1) or were shot selected for association with beads in order to facilitate larger numbers of beads to be assessed in between group comparisons of the proportion of beads attached/internalized (other figures).

MTOC/cav1 recruitment assay

For the caveolin recruitment studies MDCK II cells already expressing GFP-tubulin were transfected with plasmid cav1-RFP using the lipid based transfection reagent Fugene6 (Roche Applied Sciences). A PcDNA3.1 cav1-RFP construct (a gift from Prof. T. Wileman) (88) was subcloned into the PcDNA3.1 hygromycin vector (Invitrogen). The Cav1-RFP insert was subcloned into the PcDNA3.1hygro vector between the *Hin*dIII and *Xho*I restriction sites. The PcDNA3.1cav1-RFP/hygro plasmid was linearized prior to transfection with restriction enzyme *fsp*I.

Cells expressing both fluorescent constructs were selected for by using a combination of G418 (1 mg/mL) and hygromycin B (200 μg/mL) and subjecting the cells to monoclonal selection yielding line MDCK II GT-RC. These cells were then grown on 13 mm diameter coverslips overnight, 1.4×10^4 TcTS coated beads were incubated with the cells for a range of time points. Cells were fixed with methanol (90%):MES (10%) for 5 min and DAPI stained.

The MTOC studies were completed in the same way but cells were labelled with anti-TAT antibody to label tubulin; cells were then DAPI stained and mounted ready for imaging.

Invasion assays

Tissue culture trypomastigotes (TCTs) from the *T. cruzi* Silvio and 92101601P strains were obtained from the supernatant of infected Vero cell monolayers by centrifugation. Purified TCTs were killed by overnight treatment with amphotericin B (1 μg/mL).

MDCK II cells were seeded at a density of 1×10^4 overnight and washed with DMEM before addition of TCTs resuspended in DMEM at an MOI of 50. Trypomastigotes were incubated with MDCK II cells for 1 h before rinsing uninvaded parasites with PBS and fixed with 4% paraformaldehyde for 10 min.

Dead TCTs were centrifuged onto MDCK II cells at 300 x g for 1 min and then incubated together for 6 h at 37°C prior to fixation (as above).

Cav1 siRNA

Cav1 (Genbank Acc. No: NM_001003296) was silenced using custom siRNA sequences: GCGGAGGAGATGAGCGAGA and GCAAATACGTA-GACTCCGA (Dharmacon). Non-targeting siRNA from the on-target plus control pool (Dharmacon) was used as a control. Cells were grown to 40% confluency before transfection using JetPrime transfection reagents (Polyplus). After 24 h transfection media was replaced with either fresh

DMEM or DMEM plus TcTS coated beads. MDCK II lysates were prepared using RIPA buffer and subjected to western blot analysis using an Odyssey® infrared imager (LI-COR® Biosciences). Densitometry was done using Odyssey software by calculating the relative intensity of the loading control. TcTS coated beads were then incubated with transfected and untransfected cells for 2 h before biotinylation.

Fluorescence microscopy

The confocal microscopy was performed using a Zeiss LSM510 META, approximately 50 beads were assayed and each experiment was done in triplicate unless otherwise stated. Visualization of cav1, β-actin and tubulin was achieved using a Zeiss Axioplan 2 microscope and a Zeiss AxioCamHR camera. All image analysis was done using Axiovision 4.7 software.

Laurdan imaging

Membrane order was evaluated using the fluorescent probe 6-dodecanoyl-2-dimethylaminonapthalene (Laurdan) (Roche). Laurdan was solubilized in dimethylsulfoxide (DMSO) to a stock concentration of 1 mM and kept at room temperature in the dark. MDCK II cells were grown overnight in chamber coverglass systems (Nunc), and protein coated beads were added and centrifuged for 1 min at 300 × ***g*** to promote bead-cell contact and transferred to 4°C for 15 min. Unattached beads were then removed by rinsing with ice cold PBS and Laurdan added at 10 μM. Cells were then incubated in the dark with gentle rocking for 15 min, to allow incorporation of the probe. Cells were rinsed again with PBS and imaged immediately. For the cholesterol depletion experiment cells were incubated with 10 mM of MBCD prior to addition of beads. GP average of the cell membrane in each GP image was analysed using SimFCS software.

Transmission electron microscopy

Cells were grown on 10 cm plates until sub-confluent, whereupon protein coated beads were added and incubated with the cells overnight at 37°C. Cells then were washed in PBS and fixed with glutaraldehyde (2.5%). These cells were collected by scraping, and were pelleted at 86 × ***g***. The pellets were then stored in 2.5% glutaradehyde until processing for electron microscopy. At that point residual phosphate was removed by rinsing with 0.1 M cacodylate buffer. The pellets were then postfixed for 1 h at room temperature with 1% osmium tetroxide, 0.8% potassium ferricyanide and 5 mM calcium chloride before being further rinsed in cacodylate buffer. The cells were then dehydrated using increasing concentrations of graded acetone before embedding the pellet in Epon. Ultrathin sections were stained with uranyl acetate and lead citrate. Observations were made using a Zeiss EM-900 transmission electron microscope.

Imaging of TS coated beads (Glycan assay)

We utilized biotinylated polyacrylamido (PAA) glycans, which were purchased from Lectinity: http://www. lectinity.com/ and were dissolved in 10 mM PBS to a concentration of 1 mg/mL. One hundred microlitres of pre-coated bead suspension was aliquoted into 12 microcentrifuge tubes per protein. Each of the 10 synthesized glycans was added to the beads (10 μg) and mixed for 15 min at 4°C. Beads were then spun for 5 min at 160 × ***g*** twice and washed with PBS to remove excess glycan. The streptavidin conjugate (Cy3) was added directly to each bead suspension (0.5 μL) and incubated for 10 min at 4°C. Beads were washed with PBS, centrifuged at 160 × *g* for 10 min and 10 μL of the suspension was added to slides. Beads were imaged immediately using a Axioplan 2 (Zeiss) microscope and Axiovision 4.5 software. The glycans were numbered and keyed by another investigator so that these experiments were done blind. Beads were given a score of 0, 1 or 2, and at least 50 beads were assayed. The scores were added together and the relevance was calculated by Chi-squared analysis (SPSS).

Live/dead cell assay

Cell death was determined by the cell LIVE/DEAD assay (molecular probes, Invitrogen) as per manufacturer instruction. Imaging of the cytoskeleton and LIVE/DEAD assay was achieved using an AxioPlan 2 microscope (Zeiss), 63× objective and a AxioCamMR Camera (Zeiss).

Statistical analysis

Statistical analysis was conducted using Prism software (GraphPad Software Inc.) using an unpaired Student *t*-test; $p < 0.05$ was considered statistically significant. Unless otherwise stated graphs show the mean of triplicate experiments with ± SEM.

Acknowledgments

The authors would like to thank Profs. S. Schenkman and A.C.C. Frasch for their help and advice in working with and inhibiting trans-sialidase. Prof. W. De Souza (UFRJ, Brazil) for granting us lab space to do the TEM, Dr. Emile Barrias for helping with TEM processing, Dr. Guy Wheeler for assistance with Laurdan analysis and Dr. P. Thomas for help with all the imaging aspects of this project. We also thank Dr. M. Mogensen (UEA, UK) and Prof. P. Hunter (UEA, UK) for their help and advice about the experiments and Prof. T. Wileman (UEA, UK) for his critical review of the manuscript. This work was supported from Wellcome Trust project grant 081059/Z/06/Z.

Supporting Information

Additional Supporting Information may be found in the online version of this article:

Figure S1: Active trans-sialidase can be purified using dynabead technology. TcTS and TcTS2V0 was purified using His-tag Dynabeads®, fractions; Lysate (L), Pellet (P), Flow through (F), washes 1–4 (W) and the eluate (E) were separated by SDS–PAGE and the resultant gel was stained with SYPRO® Ruby protein gel stain (A). About 1.4×10^4 of sulphate modified latex beads were coated with 10, 15, 20, 25, 30, 35 μg of TcTS and were then separated from the beads by SDS–PAGE and analysed by western blot using anti-his antibody (B). Trans-sialidase activity was assayed by fluorometric assay where MuGal (4-methylumbelliferyl-beta-D-galactoside) acts as the acceptor substrate for the sialic acid from the 3′SL (3′sialyl lactose) donor, (C) gives activity with increasing amounts of TcTS. The activity per 20 μg of purified protein was measured in addition to protein coated beads and compared with *Trypanosoma cruzi* trypomastigote lysate (mean ± SEM, $N = 2$) (D).

Figure S2: The percentage of internalized TcTS coated beads increases with time. The percentage of internalized TcTS coated beads was plotted over an 8 h time period.

Figure S3: The TcTS and TcTS2V0 glycan binding profile. Beads coated with TcTS and TcTS2V0 were incubated with 10 synthetic glycans (key) which were then detected by microscopy using streptavidinCy3 (red) (A). The beads were then scored according to the amount of fluorescence observed and the mean score is shown in graph B, where * depicts a significant difference according to Chi-square analysis.

Figure S4: Pertussis toxin does no lead to excessive cell death. MDCK II cells were labelled using a LIVE/DEAD® cell assay kit after treatment with pertussis toxin (PT) and immediately imaged using a Zeiss Axioplan 2 microscope showing live cells in green and dead cells in red (A) scale bars are 5 μm. One hundred cells were scored dead or alive in triplicate experiments and shown in (B) (mean ± SEM, $N = 3$).

Figure S5: The MTOC migrates towards internalized TcTS coated beads. The mean distance of the MTOC from the centre of the bead was measured at a range of time points (mean ± SEM, $N = 3$; B).

Figure S6: MBCD does not lead to excessive cell death at concentrations below 20 mM. MDCK II cells treated with a range of MBCD concentrations were labelled using a LIVE/DEAD® cell assay kit

and immediately imaged using a Zeiss Axioplan 2 microscope showing live cells in green and dead cells in red (A) scale bars are 5 μm. One hundred cells were scored dead or alive in triplicate experiments and shown in (B) (mean ± SEM, $N = 3$).

Figure S7: MBCD treatment dissipates the lipid order present at the bead-cell interface. Cells were treated with the cholesterol depleting reagent, MBCD, prior to treatment with Laurdan and incubation with TcTS and TcTS2V0 coated beads. The resultant images demonstrated that for both sets of protein coated beads the cells appeared a lot bluer and in the region in contact with beads the cells no longer exhibited the yellow/orange characteristic (A). The cell surface membrane in general was a lot bluer in accordance with a loss of lipid order but this was not seen in some of the vesicles which retained their order suggesting that cholesterol is lost from the cell surface membrane. The corresponding histograms demonstrate a negative shift in the average GP to −0.098 in the presence of TcTS coated beads and to −0.019 for TcTS2V0 (B).

References

1. Hotez PJ, Dumonteil E, Woc-Colburn L, Serpa JA, Bezek S, Edwards MS, Hallmark CJ, Musselwhite LW, Flink BJ, Bottazzi ME. Chagas disease: "The New HIV/AIDS of the Americas". PLoS Negl Trop Dis 2012;6:e1498.
2. WHO. World Health Report. Geneva: World Health Organisation; 2002.
3. Brener Z. Biology of *Trypanosoma cruzi*. Annu Rev Microbiol 1973;27:347–382.
4. Tyler KM, Engman DM. The life cycle of *Trypanosoma cruzi* revisited. Int J Parasitol 2001;31(5–6):472–481.
5. Tardieux I, Nathanson MH, Andrews NW. Role in host cell invasion of *Trypanosoma cruzi*-induced cytosolic-free Ca2+ transients. J Exp Med 1994;179:1017–1022.
6. Barr SC, Han W, Andrews NW, Lopez JW, Ball BA, Pannabecker TL, Gilmour RF Jr. A factor from *Trypanosoma cruzi* induces repetitive cytosolic free Ca2+ transients in isolated primary canine cardiac myocytes. Infect Immun 1996;64:1770–1777.
7. Rodriguez A, Samoff E, Rioult MG, Chung A, Andrews NW. Host cell invasion by trypanosomes requires lysosomes and microtubule/kinesin-mediated transport. J Cell Biol 1996;134:349–362.
8. Roychowdhury S, Martinez L, Salgado L, Das S, Rasenick MM. G protein activation is prerequisite for functional coupling between Galpha/Gbetagamma and tubulin/microtubules. Biochem Biophys Res Commun 2006;340:441–448.
9. Tardieux I, Webster P, Ravesloot J, Boron W, Lunn JA, Heuser JE, Andrews NW. Lysosome recruitment and fusion are early events required for trypanosome invasion of mammalian cells. Cell 1992;71:1117–1130.
10. Tyler KM, Luxton GW, Applewhite DA, Murphy SC, Engman DM. Responsive microtubule dynamics promote cell invasion by *Trypanosoma cruzi*. Cell Microbiol 2005;7:1579–1591.
11. Butler CE, Tyler KM. Membrane traffic and synaptic cross-talk during host cell entry by *Trypanosoma cruzi*. Cell Microbiol 2012;14:1345–1353.
12. Scharfstein J, Schmitz V, Morandi V, Capella MM, Lima AP, Morrot A, Juliano L, Muller-Esterl W. Host cell invasion by *Trypanosoma cruzi* is potentiated by activation of bradykinin B(2) receptors. J Exp Med 2000;192:1289–1300.
13. Croxford JL, Wang K, Miller SD, Engman DM, Tyler KM. Effects of cannabinoid treatment on Chagas disease pathogenesis: balancing inhibition of parasite invasion and immunosuppression. Cell Microbiol 2005;7:1592–1602.
14. Rodriguez A, Martinez I, Chung A, Berlot CH, Andrews NW. cAMP regulates Ca2+-dependent exocytosis of lysosomes and lysosome-mediated cell invasion by trypanosomes. J Biol Chem 1999;274:16754–16759.
15. Fernandes MC, Cortez M, Geraldo Yoneyama KA, Straus AH, Yoshida N, Mortara RA. Novel strategy in *Trypanosoma cruzi* cell invasion: implication of cholesterol and host cell microdomains. Int J Parasitol 2007;37:1431–1441.
16. Barrias ES, Dutra JM, De Souza W, Carvalho TM. Participation of macrophage membrane rafts in *Trypanosoma cruzi* invasion process. Biochem Biophys Res Commun 2007;363:828–834.
17. Schettino PM, Majumder S, Kierszenbaum F. Regulatory effect of the level of free Ca2+ of the host cell on the capacity of *Trypanosoma cruzi* to invade and multiply intracellularly. J Parasitol 1995;81:597–602.
18. Rodriguez A, Rioult MG, Ora A, Andrews NW. A trypanosome-soluble factor induces IP3 formation, intracellular Ca2+ mobilization and microfilament rearrangement in host cells. J Cell Biol 1995;129:1263–1273.
19. Caler EV, Morty RE, Burleigh BA, Andrews NW. Dual role of signaling pathways leading to Ca(2+) and cyclic AMP elevation in host cell invasion by *Trypanosoma cruzi*. Infect Immun 2000;68:6602–6610.
20. Woolsey AM, Sunwoo L, Petersen CA, Brachmann SM, Cantley LC, Burleigh BA. Novel PI 3-kinase-dependent mechanisms of trypanosome invasion and vacuole maturation. J Cell Sci 2003;116(Pt 17):3611–3622.
21. Tam C, Idone V, Devlin C, Fernandes MC, Flannery A, He X, Schuchman E, Tabas I, Andrews NW. Exocytosis of acid sphingomyelinase by wounded cells promotes endocytosis and plasma membrane repair. J Cell Biol 2010;189:1027–1038.
22. Fernandes MC, Cortez M, Flannery AR, Tam C, Mortara RA, Andrews NW. *Trypanosoma cruzi* subverts the sphingomyelinase-mediated plasma membrane repair pathway for cell invasion. J Exp Med 2011;208:909–921.
23. Woolsey AM, Burleigh BA. Host cell actin polymerization is required for cellular retention of *Trypanosoma cruzi* and early association with endosomal/lysosomal compartments. Cell Microbiol 2004;6:829–838.
24. Gaidarov I, Smith ME, Domin J, Keen JH. The class II phosphoinositide 3-kinase C2alpha is activated by clathrin and regulates clathrin-mediated membrane trafficking. Mol Cell 2001;7:443–449.
25. Pelkmans L, Zerial M. Kinase-regulated quantal assemblies and kiss-and-run recycling of caveolae. Nature 2005;436:128–133.
26. Rothberg KG, Heuser JE, Donzell WC, Ying YS, Glenney JR, Anderson RG. Caveolin, a protein component of caveolae membrane coats. Cell 1992;68:673–682.
27. Cremona ML, Sanchez DO, Frasch AC, Campetella O. A single tyrosine differentiates active and inactive *Trypanosoma cruzi* trans-sialidases. Gene 1995;160:123–128.
28. Alves MJ, Colli W. *Trypanosoma cruzi*: adhesion to the host cell and intracellular survival. IUBMB Life 2007;59(4–5):274–279.
29. Chuenkova M, Pereira ME. *Trypanosoma cruzi* trans-sialidase: enhancement of virulence in a murine model of Chagas' disease. J Exp Med 1995;181:1693–1703.
30. Pereira ME, Zhang K, Gong Y, Herrera EM, Ming M. Invasive phenotype of *Trypanosoma cruzi* restricted to a population expressing trans-sialidase. Infect Immun 1996;64:3884–3892.
31. Yoshida N. *Trypanosoma cruzi* infection by oral route: how the interplay between parasite and host components modulates infectivity. Parasitol Int 2008;57:105–109.
32. Agusti R, Paris G, Ratier L, Frasch AC, de Lederkremer RM. Lactose derivatives are inhibitors of *Trypanosoma cruzi* trans-sialidase activity toward conventional substrates in vitro and in vivo. Glycobiology 2004;14:659–670.
33. Schenkman RP, Vandekerckhove F, Schenkman S. Mammalian cell sialic acid enhances invasion by *Trypanosoma cruzi*. Infect Immun 1993;61:898–902.
34. Ramirez MI, Ruiz Rde C, Araya JE, Da Silveira JF, Yoshida N. Involvement of the stage-specific 82-kilodalton adhesion molecule of *Trypanosoma cruzi* metacyclic trypomastigotes in host cell invasion. Infect Immun 1993;61:3636–3641.
35. Ferreira D, Cortez M, Atayde VD, Yoshida N. Actin cytoskeleton-dependent and -independent host cell invasion by *Trypanosoma cruzi* is mediated by distinct parasite surface molecules. Infect Immun 2006;74:5522–5528.
36. Rubin-de-Celis SS, Uemura H, Yoshida N, Schenkman S. Expression of trypomastigote trans-sialidase in metacyclic forms of *Trypanosoma cruzi* increases parasite escape from its parasitophorous vacuole. Cell Microbiol 2006;8:1888–1898.

37. Mucci J, Risso MG, Leguizamon MS, Frasch AC, Campetella O. The trans-sialidase from *Trypanosoma cruzi* triggers apoptosis by target cell sialylation. Cell Microbiol 2006;8:1086–1095.
38. Tonelli RR, Giordano RJ, Barbu EM, Torrecilhas AC, Kobayashi GS, Langley RR, Arap W, Pasqualini R, Colli W, Alves MJ. Role of the gp85/trans-sialidases in *Trypanosoma cruzi* tissue tropism: preferential binding of a conserved peptide motif to the vasculature in vivo. PLoS Negl Trop Dis 2011;4:e864.
39. Miyagi T, Yamaguchi K. Mammalian sialidases: physiological and pathological roles in cellular functions. Glycobiology 2012;22:880–896.
40. Florey O, Overholtzer M. Autophagy proteinsin macroendocytic engulfment. Trends Cell Biol 2012.
41. Overholtzer M, Mailleux AA, Mouneimne G, Normand G, Schnitt SJ, King RW, Cibas ES, Brugge JS. A nonapoptotic cell death process, entosis, that occurs by cell-in-cell invasion. Cell 2007;131:966–979.
42. Florey O, Kim SE, Sandoval CP, Haynes CM, Overholtzer M. Autophagy machinery mediates macroendocytic processing and entotic cell death by targeting single membranes. Nat Cell Biol 2011;13:1335–1343.
43. Linnartz B, Kopatz J, Tenner AJ, Neumann H. Sialic acid on the neuronal glycocalyx prevents complement C1 binding and complement receptor-3-mediated removal by microglia. J Neurosci 2012;32:946–952.
44. Meesmann HM, Fehr EM, Kierschke S, Herrmann M, Bilyy R, Heyder P, Blank N, Krienke S, Lorenz HM, Schiller M. Decrease of sialic acid residues as an eat-me signal on the surface of apoptotic lymphocytes. J Cell Sci 2010;123(Pt 19):3347–3356.
45. Rohloff P, Rodrigues CO, Docampo R. Regulatory volume decrease in *Trypanosoma cruzi* involves amino acid efflux and changes in intracellular calcium. Mol Biochem Parasitol 2003;126:219–230.
46. Toker A, Cantley LC. Signalling through the lipid products of phosphoinositide-3-OH kinase. Nature 1997;387:673–676.
47. Corvera S, Czech MP. Direct targets of phosphoinositide 3-kinase products in membrane traffic and signal transduction. Trends Cell Biol 1998;8:442–446.
48. Cantley LC. The phosphoinositide 3-kinase pathway. Science 2002;296:1655–1657.
49. Olianas MC, Dedoni S, Onali P. Regulation of PI3K/Akt signaling by N-desmethylclozapine through activation of delta-opioid receptor. Eur J Pharmacol 2011;660(2–3):341–350.
50. Todorov AG, Einicker-Lamas M, de Castro SL, Oliveira MM, Guilherme A. Activation of host cell phosphatidylinositol 3-kinases by *Trypanosoma cruzi* infection. J Biol Chem 2000;275:32182–32186.
51. Procopio DO, Barros HC, Mortara RA. Actin-rich structures formed during the invasion of cultured cells by infective forms of *Trypanosoma cruzi*. Eur J Cell Biol 1999;78:911–924.
52. Schenkman S, Pontes de Carvalho L, Nussenzweig V. *Trypanosoma cruzi* trans-sialidase and neuraminidase activities can be mediated by the same enzymes. J Exp Med 1992;175:567–575.
53. Simons K, Vaz WL. Model systems, lipid rafts, and cell membranes. Annu Rev Biophys Biomol Struct 2004;33:269–295.
54. Jordan S, Rodgers W. T cell glycolipid-enriched membrane domains are constitutively assembled as membrane patches that translocate to immune synapses. J Immunol 2003;171:78–87.
55. Vieira FS, Correa G, Einicker-Lamas M, Coutinho-Silva R. Host-cell lipid rafts: a safe door for micro-organisms? Biol Cell 2010;102:391–407.
56. Wheeler G, Tyler KM. Widefield microscopy for live imaging of lipid domains and membrane dynamics. Biochim Biophys Acta 2010.
57. Tyler KM, Fridberg A, Toriello KM, Olson CL, Cieslak JA, Hazlett TL, Engman DM. Flagellar membrane localization via association with lipid rafts. J Cell Sci 2009;122(Pt 6):859–866.
58. Cortez M, Neira I, Ferreira D, Luquetti AO, Rassi A, Atayde VD, Yoshida N. Infection by *Trypanosoma cruzi* metacyclic forms deficient in gp82 but expressing a related surface molecule, gp30. Infect Immun 2003;71:6184–6191.
59. Favoreto S Jr, Dorta ML, Yoshida N. *Trypanosoma cruzi* 175-kDa protein tyrosine phosphorylation is associated with host cell invasion. Exp Parasitol 1998;89:188–194.
60. Henry T, Couillault C, Rockenfeller P, Boucrot E, Dumont A, Schroeder N, Hermant A, Knodler LA, Lecine P, Steele-Mortimer O, Borg JP, Gorvel JP, Meresse S. The Salmonella effector protein PipB2 is a linker for kinesin-1. Proc Natl Acad Sci USA 2006;103:13497–13502.
61. Coppens I, Dunn JD, Romano JD, Pypaert M, Zhang H, Boothroyd JC, Joiner KA. *Toxoplasma gondii* sequesters lysosomes from mammalian hosts in the vacuolar space. Cell 2006;125:261–274.
62. Romano JD, Bano N, Coppens I. New host nuclear functions are not required for the modifications of the parasitophorous vacuole of Toxoplasma. Cell Microbiol 2008;10:465–476.
63. Friedrich N, Santos JM, Liu Y, Palma AS, Leon E, Saouros S, Kiso M, Blackman MJ, Matthews S, Feizi T, Soldati-Favre D. Members of a novel protein family containing microneme adhesive repeat domains act as sialic acid-binding lectins during host cell invasion by apicomplexan parasites. J Biol Chem 2010;285:2064–2076.
64. Friedrich N, Matthews S, Soldati-Favre D. Sialic acids: key determinants for invasion by the Apicomplexa. Int J Parasitol 2010;40:1145–1154.
65. Sinai AP, Joiner KA. The *Toxoplasma gondii* protein ROP2 mediates host organelle association with the parasitophorous vacuole membrane. J Cell Biol 2001;154:95–108.
66. Ndjamen B, Kang BH, Hatsuzawa K, Kima PE. Leishmania parasitophorous vacuoles interact continuously with the host cell's endoplasmic reticulum; parasitophorous vacuoles are hybrid compartments. Cell Microbiol 2010;12:1480–1494.
67. Romano PS, Arboit MA, Vazquez CL, Colombo MI. The autophagic pathway is a key component in the lysosomal dependent entry of *Trypanosoma cruzi* into the host cell. Autophagy 2009;5:6–18.
68. Lafont F, van der Goot FG. Bacterial invasion via lipid rafts. Cell Microbiol 2005;7:613–620.
69. Chessa D, Winter MG, Jakomin M, Baumler AJ. Salmonella enterica serotype Typhimurium Std fimbriae bind terminal alpha(1,2)fucose residues in the cecal mucosa. Mol Microbiol 2009;71:864–875.
70. Nagajyothi F, Weiss LM, Silver DL, Desruisseaux MS, Scherer PE, Herz J, Tanowitz HB. *Trypanosoma cruzi* utilizes the host low density lipoprotein receptor in invasion. PLoS Negl Trop Dis 2011;5:e953.
71. Medina FA, Cohen AW, de Almeida CJ, Nagajyothi F, Braunstein VL, Teixeira MM, Tanowitz HB, Lisanti MP. Immune dysfunction in caveolin-1 null mice following infection with *Trypanosoma cruzi* (Tulahuen strain). Microbes Infect 2007;9:325–333.
72. Chichili GR, Rodgers W. Cytoskeleton–membrane interactions in membrane raft structure. Cell Mol Life Sci 2009;66:2319–2328.
73. Schenkman S, Mortara RA. HeLa cells extend and internalize pseudopodia during active invasion by *Trypanosoma cruzi* trypomastigotes. J Cell Sci 1992;101(Pt 4):895–905.
74. Kobayashi S, Kojidani T, Osakada H, Yamamoto A, Yoshimori T, Hiraoka Y, Haraguchi T. Artificial induction of autophagy around polystyrene beads in nonphagocytic cells. Autophagy 2010;6:36–45.
75. Mercer J, Helenius A. Virus entry by macropinocytosis. Nat Cell Biol 2009;11:510–520.
76. Barrias ES, Reignault LC, De Souza W, Carvalho TM. *Trypanosoma cruzi* uses macropinocytosis as an additional entry pathway into mammalian host cell. Microbes Infect 2012.
77. Michineau S, Alhenc-Gelas F, Rajerison RM. Human bradykinin B2 receptor sialylation and N-glycosylation participate with disulfide bonding in surface receptor dimerization. Biochemistry 2006;45:2699–2707.
78. Michineau S, Muller L, Pizard A, Alhenc-Gelas F, Rajerison RM. N-linked glycosylation of the human bradykinin B2 receptor is required for optimal cell-surface expression and coupling. Biol Chem 2004;385:49–57.
79. Liu YF, Ghahremani MH, Rasenick MM, Jakobs KH, Albert PR. Stimulation of cAMP synthesis by Gi-coupled receptors upon ablation of distinct Galphai protein expression. Gi subtype specificity of the 5-HT1A receptor. J Biol Chem 1999;274:16444–16450.
80. Caler EV, Chakrabarti S, Fowler KT, Rao S, Andrews NW. The exocytosis-regulatory protein synaptotagmin VII mediates cell invasion by *Trypanosoma cruzi*. J Exp Med 2001;193:1097–1104.
81. Neira I, Silva FA, Cortez M, Yoshida N. Involvement of *Trypanosoma cruzi* metacyclic trypomastigote surface molecule gp82 in adhesion to gastric mucin and invasion of epithelial cells. Infect Immun 2003;71:557–561.
82. Liu B, Wu JM, Li J, Liu JJ, Li WW, Li CY, Xu HL, Bao JK. Polygonatum cyrtonema lectin induces murine fibrosarcoma L929 cell apoptosis and autophagy via blocking Ras-Raf and PI3K-Akt signaling pathways. Biochimie 2010;92:1934–1938.

83. Schenkman S, Chaves LB, Pontes de Carvalho LC, Eichinger D. A proteolytic fragment of *Trypanosoma cruzi* trans-sialidase lacking the carboxyl-terminal domain is active, monomeric, and generates antibodies that inhibit enzymatic activity. J Biol Chem 1994;269:7970–7975.
84. Schrader S, Tiralongo E, Paris G, Yoshino T, Schauer R. A nonradioactive 96-well plate assay for screening of trans-sialidase activity. Anal Biochem 2003;322:139–147.
85. Tsuda K, Amano A, Umebayashi K, Inaba H, Nakagawa I, Nakanishi Y, Yoshimori T. Molecular dissection of internalization of *Porphyromonas gingivalis* by cells using fluorescent beads coated with bacterial membrane vesicle. Cell Struct Funct 2005;30:81–91.
86. Cardaba CM, Kerr JS, Mueller A. CCR5 internalization and signalling have different dependence on membrane lipid raft integrity. Cell Signal 2008;20:1687–1694.
87. Ojakian GK, Schwimmer R. Antimicrotubule drugs inhibit the polarized insertion of an intracellular glycoprotein pool into the apical membrane of Madin-Darby canine kidney (MDCK) cells. J Cell Sci 1992;103(Pt 3):677–687.
88. Sharma DK, Brown JC, Choudhury A, Peterson TE, Holicky E, Marks DL, Simari R, Parton RG, Pagano RE. Selective stimulation of caveolar endocytosis by glycosphingolipids and cholesterol. Mol Biol Cell 2004;15:3114–3122.